Available online at www.sciencedirect.com
SCIENCE DIRECT®
PERGAMON
International Journal of Heat and Mass Transfer 46 (2003) 4813–4822
International Journal of HEAT and MASS TRANSFER
www.elsevier.com/locate/ijhmt

An explicit solution for the combined heat and mass transfer by natural convection from a vertical wall in a non-Darcy porous medium

Chun Wang *, Shijun Liao, Jimao Zhu

School of Naval Architecture and Ocean Engineering, Shanghai JiaoTong University, Shanghai 200030, China

Received 14 December 2002; received in revised form 29 May 2003

Abstract

An analytic technique, namely the homotopy analysis method, is applied to solve the combined heat and mass transfer by natural convection adjacent to a vertical wall in a non-Darcy porous medium governed by a set of three fully coupled, highly nonlinear similarity equations. An explicit, totally analytic and uniformly valid solution is derived, which agrees well with numerical results.

Keywords: Non-Darcy natural convection; Porous medium; Analytic solution; Homotopy analysis method

1. Introduction

Combined heat and mass transfer driven by buoyancy due to temperature and concentration is of practical importance, since there are many possible engineering applications, such as the migration of moisture through the air contained in fibrous insulations and grain storage installations, and dispersion of chemical contaminants through water-saturated soil. The state of art concerning combined heat and mass transfer in porous media has been summarized in the excellent monographs by Nield and Bejan [1].

A number of studies have been reported in the literature focusing on the problem of combined heat and mass transfer in porous media. Nield [2] made the first attempt to study the stability of convective flow in horizontal layers with imposed vertical temperature and concentration gradients. This was followed by Khan and Zebib [3] in the study of flow stability in a vertical porous layer. Jang and Chang [4] analyzed the vortex instability along a horizontal surface by considering boundary layer flows. Raptis et al. [5,6] presented a series solution considering wall-shear and suction for boundary layer flows with different wall conditions. For a vertical plate in a saturated porous medium, Bejan and Khair [7] reported similarity solutions for the special case of a wall with constant temperature and concentration. This fundamental case was also treated by Nakayama and Hossain [8] and Singh and Queeny [9] using an integral method. Lai and Kulacki [10] considered another important case of a wall with constant heat and mass flux including the effect of wall injection. The dispersion and opposing buoyancy effects were analyzed by Telles and Trevisan [11] and Angirasa et al. [12], respectively. Natural convection in porous media with combined buoyancy effects for other geometries were studied by Trevisan and Bejan [13,14], Hasan and Mujumdar [15], Jang and Chang [16], Lai et al. [17]. In addition to the previous studies for steady cases, unsteady flows were also extensively studied by Raptis [18], Jang and Ni [19], Kumari and Nath [20], and Pop and Herwig [21]. A good literature review on the phenomena has been recently provided by Trevisan and Bejan [22].

Relative to the above research activities on Darcy flow driven by double buoyancy effects, the works on non-Darcy flow driven by two buoyancy effects are quite limited. Kumari et al. [23] focused on the free convection

* Corresponding author.
E-mail addresses: chunwang@sjtu.edu.cn (C. Wang), sjliao@sjtu.edu.cn (S. Liao), jmzhu@sjtu.edu.cn (J. Zhu).

0017-9310/$ - see front matter
doi:10.1016/S0017-9310(03)00347-8

from axisymmetric bodies of arbitray shape, while Jang et al. [24] addressed on that from a vertical wall. Double-diffusion from a vertical surface in a porous region saturated within a non-Newtonian fluid was studied by Rastogi and Poulikakos [25]. Recently, based on Forchheimer flow model, Murthy and Singh [26] studied the effect of lateral mass flux on the free convection heat and mass transfer from a vertical wall in a fluid saturated porous medium.

Due to its important applications in many fields described by Nield and Bejan [1], a full understanding for combined heat and mass transfer by non-Darcy natural convection from a heated flat surface embedded in fluid-saturated porous medium is meaningful. Although numerical results have been reported by Murthy and Singh [26], to our knowledge, no one has reported an explicit, totally analytic, uniformly valid solution for this problem. In this paper, we employ the homotopy analysis method (HAM) [27–33] to give such an explicit analytic solution. It is expected that the solution thus obtained will have useful applications in practice and will serve as a complement to the existing literature.

2. Governing equations

Consider a vertical flat plate embedded in a saturated porous medium as shown in Fig. 1. The plate may be permeable ($v_w \neq 0$) or impermeable ($v_w = 0$). The surface of the plate is maintained at a constant temperature T_w higher than its ambient temperature T_∞, and at the same time the concentration of a constituent decreases from C_w at the wall to C_∞ sufficiently away from the wall. Having invoked the Boussinesq and boundary-layer approximations, the governing equations based on the Forchheimer's formulation are given as by [26]

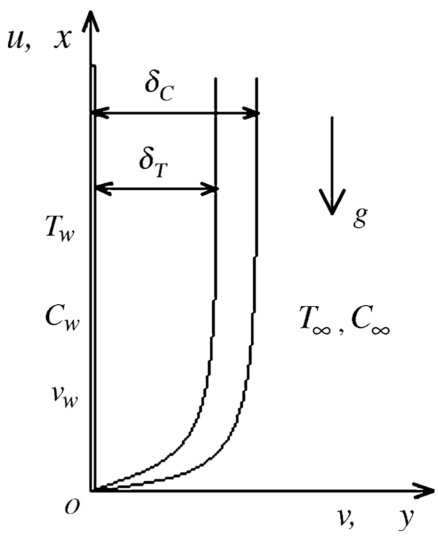

Fig. 1. Coordinate system.

$$\frac{\partial u}{\partial x} + \frac{\partial v}{\partial y} = 0, \tag{1}$$

$$\frac{\partial u}{\partial y} + \frac{c\sqrt{K}}{\nu}\frac{\partial u^2}{\partial y} = \frac{Kg}{\nu}\left(\beta_T \frac{\partial T}{\partial y} + \beta_C \frac{\partial C}{\partial y}\right), \tag{2}$$

$$u\frac{\partial T}{\partial x} + v\frac{\partial T}{\partial y} = \alpha \frac{\partial^2 T}{\partial y^2}, \tag{3}$$

$$u\frac{\partial C}{\partial x} + v\frac{\partial C}{\partial y} = D\frac{\partial^2 C}{\partial y^2}, \tag{4}$$

where (x, y) are the non-dimensional Cartesian coordinates along and normal to the flat surface, u and v are the velocity components in x- and y-directions, respectively, T is the temperature, C is the concentration, δ_T and δ_C are the thermal boundary layer thickness and the concentration boundary layer thickness, β_T is the coefficient of thermal expansion, β_C is the coefficient of concentration expansion, ν is the kinematic viscosity of the fluid, K is the permeability constant, c is an empirical constant, g is the gravity acceleration, α and D are the thermal and solutal diffusivities, respectively.

The boundary conditions to be considered are

$$y = 0: \quad v = v_w, \quad T = T_w, \quad C = C_w, \tag{5}$$

$$y \to \infty: \quad u = 0, \quad T = T_\infty, \quad C = C_\infty, \tag{6}$$

where $v_w = Ex^{-1/2}$, E is a real constant.

Under the transformation

$$\eta = \frac{y}{x} Ra_x^{1/2}, \tag{7}$$

$$u = \frac{\alpha}{x} Ra_x f'(\eta), \tag{8}$$

$$v = -\frac{\alpha}{2x} Ra_x^{1/2}(f - \eta f'), \tag{9}$$

$$\theta(\eta) = \frac{T - T_\infty}{T_w - T_\infty}, \tag{10}$$

$$\phi(\eta) = \frac{C - C_\infty}{C_w - C_\infty}, \tag{11}$$

where Ra_x is the modified Rayleigh number defined by

$$Ra_x = \frac{Kg\beta_T(T_w - T_\infty)x}{\alpha\nu}, \tag{12}$$

one has

$$f'' + 2Grf'f'' = \theta' + Br\phi', \tag{13}$$

$$\theta'' = -\frac{1}{2} f\theta', \tag{14}$$

$$\phi'' = -\frac{1}{2} Lef\phi', \tag{15}$$

subject to the boundary conditions

$$f(0) = f_w, \quad \theta(0) = \phi(0) = 1, \tag{16}$$

$$f'(\infty) = \theta(\infty) = \phi(\infty) = 0, \tag{17}$$

where

$$Gr = \frac{c\sqrt{K}Kg\beta_T(T_w - T_\infty)}{\nu^2}, \tag{18}$$

$$Br = \frac{\beta_C(C_w - C_\infty)}{\beta_T(T_w - T_\infty)}, \tag{19}$$

$$Le = \frac{\alpha}{D}, \tag{20}$$

$$f_w = -\frac{2E}{\sqrt{\alpha Kg\beta_T(T_w - T_\infty)}} \tag{21}$$

are the Grashof number, the buoyancy ratio, the Lewis number and the mass flux parameter, respectively.

3. Explicit analytic solution given by the HAM

Due to the boundary conditions (16) and (17), $f(\eta)$, $\theta(\eta)$ and $\phi(\eta)$ can be expressed in the following forms

$$f(\eta) = \sum_{n=0}^{+\infty} A_n \exp(-n\gamma\eta), \tag{22}$$

$$\theta(\eta) = \sum_{n=1}^{+\infty} B_n \exp(-n\gamma\eta), \tag{23}$$

$$\phi(\eta) = \sum_{n=1}^{+\infty} C_n \exp(-n\gamma\eta), \tag{24}$$

respectively, where A_n, B_n and C_n are coefficients to be determined, γ is a positive constant to be chosen. Then, due to (16) and (17), it is straightforward to choose

$$f_0(\eta) = 1 + f_w - \exp(-\gamma\eta), \tag{25}$$

$$\theta_0(\eta) = \frac{\exp(-\gamma\eta) + \exp(-2\gamma\eta)}{2}, \tag{26}$$

$$\phi_0(\eta) = \frac{\exp(-\gamma\eta) + \exp(-2\gamma\eta)}{2} \tag{27}$$

as the initial approximations of $f(\eta)$, $\theta(\eta)$ and $\phi(\eta)$, respectively. Furthermore, we choose

$$L_1 = \frac{\partial^2}{\partial\eta^2} - \frac{\partial}{\partial\eta}, \tag{28}$$

$$L_2 = \exp(\gamma\eta)\left(\frac{\partial^2}{\partial\eta^2} - 1\right), \tag{29}$$

as our auxiliary linear operators, which have the following properties

$$L_1[C_1 + C_2\exp(\eta)] = 0, \tag{30}$$

$$L_2[C_3\exp(-\eta) + C_4\exp(\eta)] = 0, \tag{31}$$

where C_1, C_2, C_3 and C_4 are integral constants.

Then, we construct the so-called zeroth-order deformation equations

$$(1-p)L_1[F(\eta;p) - f_0(\eta)] = p\hbar_f N_f[F(\eta;p), \Theta(\eta;p), \Phi(\eta;p)], \tag{32}$$

$$(1-p)L_2[\Theta(\eta;p) - \theta_0(\eta)] = p\hbar_\theta N_\theta[F(\eta;p), \Theta(\eta;p)], \tag{33}$$

$$(1-p)L_2[\Phi(\eta;p) - \phi_0(\eta)] = p\hbar_\phi N_\phi[F(\eta;p), \Phi(\eta;p)], \tag{34}$$

subject to the boundary conditions

$$F(0;p) = f_w, \quad \Theta(0;p) = \Phi(0;p) = 1, \tag{35}$$

$$\left.\frac{\partial F(\eta;p)}{\partial\eta}\right|_{\eta=\infty} = \Theta(\infty;p) = \Phi(\infty;p) = 0, \tag{36}$$

under the definitions

$$N_f[F,\Theta,\Phi] = \frac{\partial^2 F}{\partial\eta^2} + 2Gr\frac{\partial F}{\partial\eta}\frac{\partial^2 F}{\partial\eta^2} - \frac{\partial\Theta}{\partial\eta} - Br\frac{\partial\Phi}{\partial\eta}, \tag{37}$$

$$N_\theta[F,\Theta] = \frac{\partial^2\Theta}{\partial\eta^2} + \frac{1}{2}F\frac{\partial\Theta}{\partial\eta}, \tag{38}$$

$$N_\phi[F,\Phi] = \frac{\partial^2\Phi}{\partial\eta^2} + \frac{1}{2}LeF\frac{\partial\Phi}{\partial\eta}, \tag{39}$$

where $p \in [0,1]$ is an embedding parameter, $\hbar_f$, $\hbar_\theta$ and $\hbar_\phi$ are the auxiliary non-zero parameters. Obviously,

$$F(\eta;0) = f_0(\eta), \quad \Theta(\eta;0) = \theta_0(\eta), \quad \Phi(\eta;0) = \phi_0(\eta) \tag{40}$$

and

$$F(\eta;1) = f(\eta), \quad \Theta(\eta;1) = \theta(\eta), \quad \Phi(\eta;1) = \phi(\eta), \tag{41}$$

when $p = 0$ and $p = 1$, respectively.

We expand $F(\eta;p)$, $\Theta(\eta;p)$ and $\Phi(\eta;p)$ in Taylor's power series at $p = 0$, say

$$F(\eta;p) = F(\eta;0) + \sum_{m=1}^{+\infty} f_m(\eta)p^m, \tag{42}$$

$$\Theta(\eta;p) = \Theta(\eta;0) + \sum_{m=1}^{+\infty} \theta_m(\eta)p^m, \tag{43}$$

$$\Phi(\eta;p) = \Phi(\eta;0) + \sum_{m=1}^{+\infty} \phi_m(\eta)p^m, \tag{44}$$

where

$$f_m(\eta) = \frac{1}{m!}\left.\frac{\partial^m F(\eta;p)}{\partial p^m}\right|_{p=0}, \tag{45}$$

$$\theta_m(\eta) = \frac{1}{m!}\frac{\partial^m \Theta(\eta;p)}{\partial p^m}\bigg|_{p=0}, \tag{46}$$

$$\phi_m(\eta) = \frac{1}{m!}\frac{\partial^m \Phi(\eta;p)}{\partial p^m}\bigg|_{p=0}. \tag{47}$$

Note that the convergence regions of the series (42)–(44) are dependent upon the auxiliary parameter $\hbar_f$, $\hbar_\theta$ and $\hbar_\phi$. If the auxiliary parameters $\hbar_f$, $\hbar_\theta$ and $\hbar_\phi$ are properly chosen so that the series (42)–(44) are convergent at $p = 1$, we have due to (40) and (41) that

$$f(\eta) = f_0(\eta) + \sum_{m=1}^{+\infty} f_m(\eta), \tag{48}$$

$$\theta(\eta) = \theta_0(\eta) + \sum_{m=1}^{+\infty} \theta_m(\eta), \tag{49}$$

$$\phi(\eta) = \phi_0(\eta) + \sum_{m=1}^{+\infty} \phi_m(\eta). \tag{50}$$

Differentiating the Eqs. (32)–(34) m times with respect to p and then setting $p = 0$ and finally dividing them by $m!$, we obtain the so-called mth-order deformation equations for $f_m(\eta)$, $\theta_m(\eta)$ and $\phi_m(\eta)$ (for details, please refer to Liao [30,31])

$$L_f[f_m(\eta) - \chi_m f_{m-1}(\eta)] = \hbar_f R_m(\eta), \tag{51}$$

$$L_\theta[\theta_m(\eta) - \chi_m \theta_{m-1}(\eta)] = \hbar_\theta S_m(\eta), \tag{52}$$

$$L_\phi[\phi_m(\eta) - \chi_m \phi_{m-1}(\eta)] = \hbar_\phi W_m(\eta), \tag{53}$$

subject to the boundary conditions

$$f_m(0) = 0, \quad \theta_m(0) = \phi_m(0) = 0, \tag{54}$$

$$f'_m(\infty) = \theta_m(\infty) = \phi_m(\infty) = 0, \tag{55}$$

under the definitions

$$R_m(\eta) = f''_{m-1}(\eta) - \theta_{m-1}(\eta) - Br\phi'_{m-1}(\eta) + 2Gr\sum_{n=0}^{m-1} f'_n(\eta) f''_{m-1-n}(\eta), \tag{56}$$

$$S_m(\eta) = \theta''_{m-1}(\eta) + \frac{1}{2}\sum_{n=0}^{m-1} f_n(\eta)\theta'_{m-1-n}(\eta), \tag{57}$$

$$W_m(\eta) = \phi''_{m-1}(\eta) + \frac{1}{2}Le\sum_{n=0}^{m-1} f_n(\eta)\phi'_{m-1-n}(\eta) \tag{58}$$

and

$$\chi_m = \begin{cases} 0, & m = 1, \\ 1, & m > 1. \end{cases} \tag{59}$$

It is found that $f_m(\eta)$, $\theta_m(\eta)$ and $\phi_m(\eta)$ governed by (51)–(55) can be expressed by

$$f_m(\eta) = \sum_{k=0}^{2m+1} a_{m,k}\exp(-k\gamma\eta), \tag{60}$$

$$\theta_m(\eta) = \sum_{k=1}^{2m+2} b_{m,k}\exp(-k\gamma\eta), \tag{61}$$

$$\phi_m(\eta) = \sum_{k=1}^{2m+2} c_{m,k}\exp(-k\gamma\eta) \tag{62}$$

for $m \geqslant 1$, where $a_{m,k}$, $b_{m,k}$ and $c_{m,k}$ are coefficients. Substituting above expressions into (51)–(55), we have the recursive formulae

$$a_{m,k} = \frac{\hbar_f}{k(k+1)\gamma^2}\Gamma_{m,k} + \chi_m\lambda_{m-1,k+1}a_{m-1,k} \quad \text{for } 1 \leqslant k \leqslant 2m+1, \tag{63}$$

$$a_{m,0} = -\sum_{k=1}^{2m+1} a_{m,k}, \tag{64}$$

$$b_{m,k} = \frac{\hbar_\theta}{\gamma^2(k^2-1)}\Delta_{m,k-1} + \chi_m\lambda_{m-1,k}b_{m-1,k} \quad \text{for } 2 \leqslant k \leqslant 2m+2, \tag{65}$$

$$b_{m,1} = -\sum_{k=2}^{2m+2} b_{m,k}, \tag{66}$$

$$c_{m,k} = \frac{\hbar_\phi}{\gamma^2(k^2-1)}\Lambda_{m,k-1} + \chi_m\lambda_{m-1,k}c_{m-1,k} \quad \text{for } 2 \leqslant k \leqslant 2m+2, \text{ and} \tag{67}$$

$$c_{m,1} = -\sum_{k=2}^{2m+2} c_{m,k}, \tag{68}$$

where

$$\Gamma_{m,k} = \lambda_{m-1,k+1}a_{m-1,k}(k\gamma)^2 + \lambda_{m-1,k}(b_{m-1,k} + Brc_{m-1,k})(k\gamma) + \beta_{m,k}, \tag{69}$$

$$\Delta_{m,k} = \lambda_{m-1,k}b_{m-1,k}(k\gamma)^2 + \vartheta_{m,k}, \tag{70}$$

$$\Lambda_{m,k} = \lambda_{m-1,k}c_{m-1,k}(k\gamma)^2 + \varphi_{m,k} \quad \text{for } 1 \leqslant k \leqslant 2m+1, \text{ under the definitions} \tag{71}$$

$$\beta_{m,k} = 2Gr\sum_{n=0}^{m-1}\sum_{s=\max\{1,k-2n-1\}}^{\min\{2m-2n-1,k-1\}} (s-k)s^2\gamma^3 a_{n,k-s}a_{m-1-n,s} \quad \text{for } 2 \leqslant k \leqslant 2m, \tag{72}$$

$$\beta_{m,1} = 0, \tag{73}$$

$$\beta_{m,2m+1} = 0, \tag{74}$$

$$\vartheta_{m,k} = -\frac{1}{2}\sum_{n=0}^{m-1}\sum_{s=\max\{1,k-2n-1\}}^{\min\{2m-2n,k\}} \gamma s a_{n,k-s}b_{m-1-n,s} \quad \text{for } 1 \leqslant k \leqslant 2m+1, \tag{75}$$

$$\varphi_{m,k} = -\frac{Le}{2}\sum_{n=0}^{m-1}\sum_{s=\max\{1,k-2n-1\}}^{\min\{2m-2n,k\}} \gamma s a_{n,k-s} c_{m-1-n,s}$$

for $1 \leqslant k \leqslant 2m+1$, and (76)

$$\lambda_{m,k} = \begin{cases} 1, & 1 \leqslant k \leqslant 2m+2, \\ 0, & \text{otherelse}. \end{cases} \quad (77)$$

Using above recursive formulae, we can calculate all coefficients $a_{m,k}$, $b_{m,k}$ and $c_{m,k}$ by using only the first six

$$a_{0,0} = 1 + f_w, \quad a_{0,1} = -1, \quad b_{0,1} = b_{0,2} = c_{0,1} = c_{0,2} = \frac{1}{2}, \quad (78)$$

given by the initial approximations (25)–(27). The corresponding Mth-order approximations of (48)–(50) are

$$f(\eta) \approx f_0(\eta) + \sum_{m=1}^{M} f_m(\eta) = \sum_{m=0}^{M}\sum_{k=0}^{2m+1} a_{m,k}\exp(-k\gamma\eta), \quad (79)$$

$$\theta(\eta) \approx \theta_0(\eta) + \sum_{m=1}^{M} \theta_m(\eta) = \sum_{m=0}^{M}\sum_{k=1}^{2m+2} b_{m,k}\exp(-k\gamma\eta), \quad (80)$$

$$\phi(\eta) \approx \phi_0(\eta) + \sum_{m=1}^{M} \phi_m(\eta) = \sum_{m=0}^{M}\sum_{k=1}^{2m+2} c_{m,k}\exp(-k\gamma\eta). \quad (81)$$

When $M \to +\infty$, we have an *explicit*, *totally analytic* solution of (13)–(17).

4. Validation of the explicit analytic solution

In this section, we verify our analytic solutions by the numerical integration using the fourth-order Runge–Kutta method and Newton–Raphson technique. The initial guesses of the numerical solutions are given by f_0, θ_0 and ϕ_0, defined by Eqs. (25)–(27), respectively. To satisfy the boundary conditions at infinity, an integration distance $\eta_\infty = 40$, which was discretized into 10 000 intervals, was found to be adequate. The iterative integration procedure was repeated until the RMS error for each discretized Eqs. (13)–(15) are not greater than 5×10^{-6}.

Note that our explicit analytic solution contains the auxiliary parameters $\hbar_f$, $\hbar_\theta$, $\hbar_\phi$ and γ, which we have great freedom to choose. This provides us with a simple way to ensure the convergence of the series (48)–(50), as pointed out by Liao and his co-authors [29–33]. The parameters used for the analytic solution are listed in Table 1.

Analytic solutions of different order of approximation in case of $Gr = 1$, $Br = 1$, $f_w = 1$ and $Le = 2$ are shown in Tables 2–4, compared with numerical results. It is found that our analytic approximations agree well with the numerical ones so long as the order of approximation is high enough.

The non-dimensional velocity component in the x-direction $f'(\eta)$, temperature distribution $\theta(\eta)$ and concentration distribution $\phi(\eta)$ for varing mass flux parameter are plotted in Figs. 2–4 when $Gr = 1$, $Br = 4$, $Le = 2$. Analytic solutions for another important case of fixing $Gr = 1$, $Br = 1$, $Le = 4$ are shown in Figs. 5–7. All of them clearly indicate the very good agreement between the analytic solutions and the numerical results.

The local heat and mass fluxes from the wall are given as by [26]

$$q = -k\left.\frac{\partial T}{\partial y}\right|_{y=0} \quad (82)$$

and

$$m = -D\left.\frac{\partial C}{\partial y}\right|_{y=0}, \quad (83)$$

Table 1
Parameters used in our analytic approach

Gr	Br	f_w	Le	$\hbar_f$	$\hbar_\theta$	$\hbar_\phi$	γ	Order M
1	4	1	2	−0.4	−1.5	−1.5	1.2	60
1	4	0	2	−0.4	−1.5	−1.0	1.1	60
1	4	−1	2	−0.3	−0.8	−0.6	0.7	60
1	1	1	4	−0.5	−1.5	−0.8	1.0	60
1	1	0	4	−0.6	−1.5	−1.5	0.8	60
1	1	−1	4	−0.5	−1.5	−0.6	0.7	80
1	10	1	2	−0.3	−1.5	−0.6	1.0	80
1	10	0	2	−0.2	−1.5	−1.0	1.2	80
1	10	−1	2	−0.1	−0.5	−0.1	0.7	80
1	1	1	10	−0.3	−1.5	−0.2	1.2	80
1	1	0	10	−0.7	−1.0	−0.4	0.8	80
1	1	−1	10	−0.6	−1.0	−0.6	1.0	100

Table 2
Analytical results of $f'(\eta)$ at different order of approximation compared with numeric results in case of $Gr = 1$, $Br = 1$, $f_w = 1$, $Le = 2$

η	10 order	20 order	30 order	40 order	50 order	60 order	80 order	100 order	Numeric results
0	1.0020	1.0009	1.0001	1.0000	1.0000	1.0000	1.0000	1.0000	1.0000
0.5	0.6785	0.6716	0.6702	0.6700	0.6700	0.6700	0.6700	0.6700	0.6699
1	0.4378	0.4278	0.4261	0.4259	0.4258	0.4258	0.4258	0.4258	0.4257
1.5	0.2739	0.2636	0.2619	0.2617	0.2617	0.2617	0.2616	0.2616	0.2614
2	0.1681	0.1594	0.1580	0.1578	0.1578	0.1577	0.1577	0.1577	0.1575
2.5	0.1022	0.0956	0.0944	0.0943	0.0942	0.0942	0.0942	0.0941	0.0939
3	0.0618	0.0572	0.0563	0.0562	0.0561	0.0561	0.0560	0.0560	0.0557
3.5	0.0374	0.0343	0.0336	0.0335	0.0335	0.0334	0.0334	0.0333	0.0330
4	0.0226	0.0206	0.0201	0.0201	0.0200	0.0200	0.0199	0.0198	0.0196
4.5	0.0137	0.0124	0.0121	0.0120	0.0120	0.0120	0.0119	0.0119	0.0116
5	0.0083	0.0075	0.0073	0.0073	0.0072	0.0072	0.0072	0.0071	0.0069
5.5	0.0050	0.0045	0.0044	0.0044	0.0044	0.0043	0.0043	0.0043	0.0041
6	0.0031	0.0027	0.0027	0.0027	0.0026	0.0026	0.0026	0.0026	0.0025
6.5	0.0019	0.0017	0.0016	0.0016	0.0016	0.0016	0.0016	0.0016	0.0015
7	0.0011	0.0010	0.0010	0.0010	0.0010	0.0010	0.0010	0.0009	0.0009
7.5	0.0007	0.0006	0.0006	0.0006	0.0006	0.0006	0.0006	0.0006	0.0005
8	0.0004	0.0004	0.0004	0.0004	0.0004	0.0004	0.0004	0.0003	0.0003

Table 3
Analytical results of $\theta(\eta)$ at different order of approximation compared with numeric results in case of $Gr = 1$, $Br = 1$, $f_w = 1$, $Le = 2$

η	10 order	20 order	30 order	40 order	50 order	60 order	80 order	100 order	Numeric results
0	1.0000	1.0000	1.0000	1.0000	1.0000	1.0000	1.0000	1.0000	1.0000
0.5	0.6544	0.6563	0.6569	0.6571	0.6571	0.6571	0.6571	0.6571	0.6569
1	0.4109	0.4138	0.4147	0.4150	0.4150	0.4150	0.4150	0.4149	0.4147
1.5	0.2512	0.2541	0.2552	0.2554	0.2555	0.2555	0.2554	0.2554	0.2551
2	0.1513	0.1537	0.1546	0.1548	0.1549	0.1549	0.1548	0.1547	0.1544
2.5	0.0907	0.0922	0.0929	0.0930	0.0931	0.0931	0.0930	0.0929	0.0926
3	0.0544	0.0553	0.0556	0.0557	0.0557	0.0557	0.0556	0.0555	0.0552
3.5	0.0327	0.0332	0.0333	0.0334	0.0333	0.0333	0.0332	0.0332	0.0328
4	0.0197	0.0199	0.0200	0.0200	0.0200	0.0200	0.0199	0.0198	0.0195
4.5	0.0119	0.0120	0.0121	0.0121	0.0120	0.0120	0.0119	0.0119	0.0116
5	0.0072	0.0073	0.0073	0.0073	0.0072	0.0072	0.0072	0.0071	0.0069
5.5	0.0044	0.0044	0.0044	0.0044	0.0044	0.0044	0.0043	0.0043	0.0041
6	0.0026	0.0027	0.0027	0.0027	0.0026	0.0026	0.0026	0.0026	0.0025
6.5	0.0016	0.0016	0.0016	0.0016	0.0016	0.0016	0.0016	0.0016	0.0015
7	0.0010	0.0010	0.0010	0.0010	0.0010	0.0010	0.0010	0.0009	0.0009
7.5	0.0006	0.0006	0.0006	0.0006	0.0006	0.0006	0.0006	0.0006	0.0005
8	0.0004	0.0004	0.0004	0.0004	0.0004	0.0004	0.0004	0.0003	0.0003

where k is the thermal conductivity of the porous medium. With the aid of Eqs. (7), (10) and (11), Eqs. (82) and (83) can be rewritten as

$$q = -k(T_w - T_\infty)\frac{1}{x}Ra_x^{1/2}\theta'(0), \tag{84}$$

$$m = -D(C_w - C_\infty)\frac{1}{x}Ra_x^{1/2}\phi'(0). \tag{85}$$

From the definitions of the local Nusselt number and Sherwood number

$$Nu = \frac{qx}{k(T_w - T_\infty)}, \tag{86}$$

$$Sh = \frac{mx}{D(C_w - C_\infty)} \tag{87}$$

and with the aid of Eqs. (84) and (85), the non-dimensional heat transfer coefficient and the non-dimensional mass transfer coefficient can be written as

$$\frac{Nu}{\sqrt{Ra_x}} = -\theta'(0), \tag{88}$$

Table 4
Analytical results of $\phi(\eta)$ at different order of approximation compared with numeric results in case of $Gr = 1$, $Br = 1$, $f_w = 1$, $Le = 2$

η	10 order	20 order	30 order	40 order	50 order	60 order	80 order	100 order	Numeric results
0	1.0000	1.0000	1.0000	1.0000	1.0000	1.0000	1.0000	1.0000	1.0000
0.5	0.4762	0.4637	0.4621	0.4618	0.4617	0.4617	0.4617	0.4617	0.4618
1	0.2105	0.1946	0.1926	0.1922	0.1921	0.1921	0.1921	0.1921	0.1922
1.5	0.0910	0.0769	0.0751	0.0747	0.0746	0.0746	0.0746	0.0746	0.0747
2	0.0400	0.0295	0.0281	0.0278	0.0277	0.0277	0.0277	0.0277	0.0278
2.5	0.0184	0.0112	0.0103	0.0101	0.0100	0.0100	0.0100	0.0100	0.0101
3	0.0089	0.0043	0.0037	0.0036	0.0035	0.0035	0.0035	0.0036	0.0036
3.5	0.0046	0.0017	0.0013	0.0012	0.0012	0.0012	0.0012	0.0012	0.0013
4	0.0025	0.0007	0.0004	0.0004	0.0004	0.0004	0.0004	0.0004	0.0004
4.5	0.0014	0.0003	0.0001	0.0001	0.0001	0.0001	0.0001	0.0001	0.0002
5	0.0008	0.0001	0.0000	0.0000	0.0000	0.0000	0.0000	0.0000	0.0001
5.5	0.0005	0.0001	0.0000	0.0000	0.0000	0.0000	0.0000	0.0000	0.0000
6	0.0003	0.0000	0.0000	0.0000	0.0000	0.0000	0.0000	0.0000	0.0000
6.5	0.0002	0.0000	0.0000	0.0000	0.0000	0.0000	0.0000	0.0000	0.0000
7	0.0001	0.0000	0.0000	0.0000	0.0000	0.0000	0.0000	0.0000	0.0000
7.5	0.0001	0.0000	0.0000	0.0000	0.0000	0.0000	0.0000	0.0000	0.0000
8	0.0000	0.0000	0.0000	0.0000	0.0000	0.0000	0.0000	0.0000	0.0000

$$\frac{Sh}{\sqrt{Ra_x}} = -\phi'(0). \tag{89}$$

The Analytic values of $\theta'(0)$ and $\phi'(0)$ against Br, Le and f_w are as shown in Figs. 8–11. The analytic solutions agree well with numerical results given by Murthy and Singh [26]. It should be pointed out that Murthy and Singh had presented numerical results for Lewis number Le ranged from 0.1 to 500. However, we find that higher order of approximation is needed when $Le > 10$. Due to the capacity of our computer, we are unable to give accurate enough analytic solutions for $Le > 10$ at present, although, theoretically speaking, our analytic solution is valid for any combination of Gr, Br, f_w and Le so long as the parameter $\hbar_f$, $\hbar_\theta$, $\hbar_\phi$ and γ are properly selected and the order of approximation is high enough. Even though, our analytic solution agree well with numerical results for a wide range of the governing parameters, as shown in Figs. 8–11. All of the numerical results verify that our analytic solution is uniformly valid.

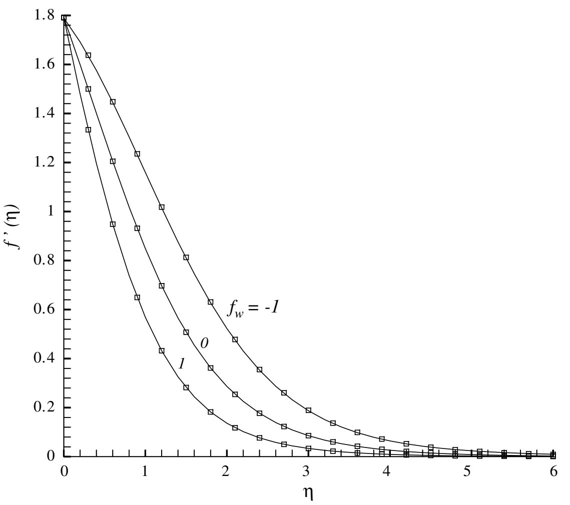

Fig. 2. Analytic results of $f'(\eta)$ compared with numerical ones when $Gr = 1$, $Br = 4$, $Le = 2$. Symbol: numerical results; solid line: homotopy analysis results.

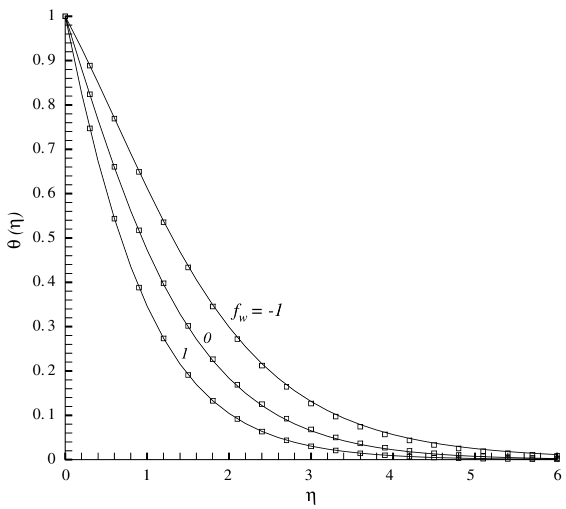

Fig. 3. Analytic results of $\theta(\eta)$ compared with numerical ones when $Gr = 1$, $Br = 4$, $Le = 2$. Symbol: numerical results; solid line: homotopy analysis results.

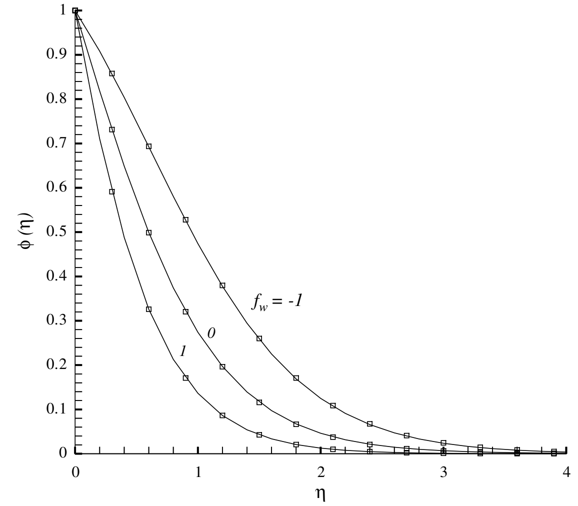

Fig. 4. Analytic results of $\phi(\eta)$ compared with numerical ones when $Gr = 1$, $Br = 4$, $Le = 2$. Symbol: numerical results; solid line: homotopy analysis results.

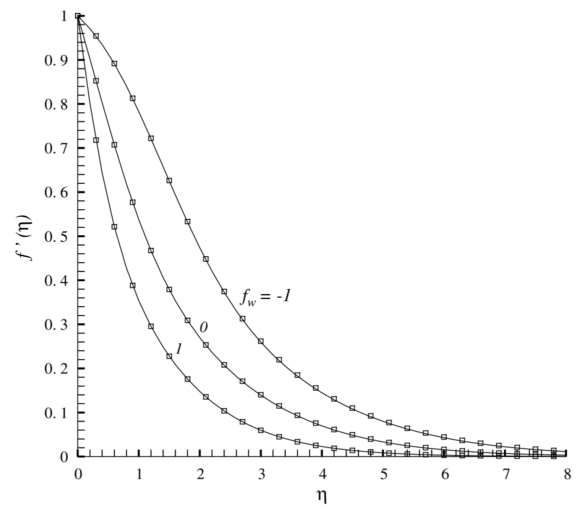

Fig. 5. Analytic results of $f'(\eta)$ compared with numerical ones when $Gr = 1$, $Br = 1$, $Le = 4$. Symbol: numerical results; solid line: homotopy analysis results.

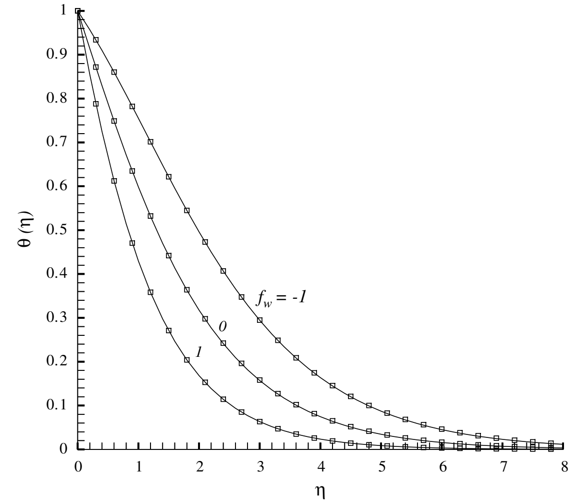

Fig. 6. Analytic results of $\theta(\eta)$ compared with numerical ones when $Gr = 1$, $Br = 1$, $Le = 4$. Symbol: numerical results; solid line: homotopy analysis results.

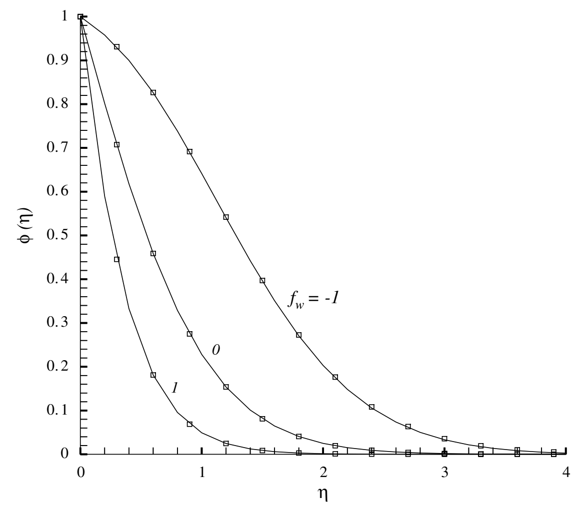

Fig. 7. Analytic results of $\phi(\eta)$ compared with numerical ones when $Gr = 1$, $Br = 1$, $Le = 4$. Symbol: numerical results; solid line: homotopy analysis results.

5. Conclusions

In this paper, we apply the homotopy analysis method [27–33] to obtain an explicit, totally analytic, uniformly valid solution of a set of three fully coupled, highly nonlinear similarity equations appeared in combined heat and mass transfer by non-Darcy free convection in porous medium (see [26]). The validity of our analytic solution is verified by numerical results. To the best of authors' knowledge, such kind of analytic solution has never been reported. This explicit analytic solution might find wide applications in engineering, such as the migration of moisture through the air contained in fibrous insulations and grain storage installations, and dispersion of chemical contaminants through water-saturated soil.

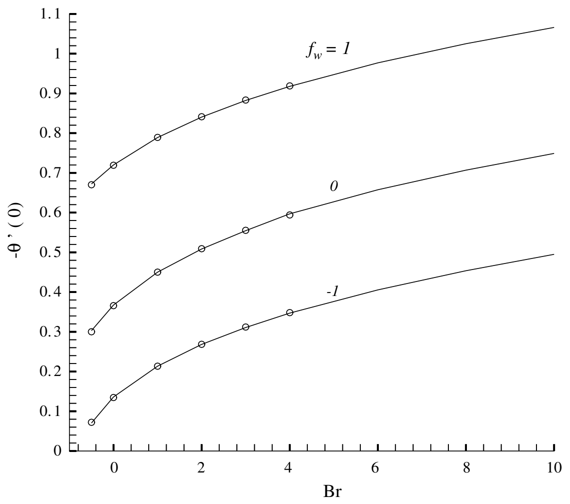

Fig. 8. The effect of buoyancy ratio Br on the Nusselts number when $Gr = 1$, $Le = 2$. Symbol: numerical results given by Murthy and Singh [26]; solid line: homotopy analysis results.

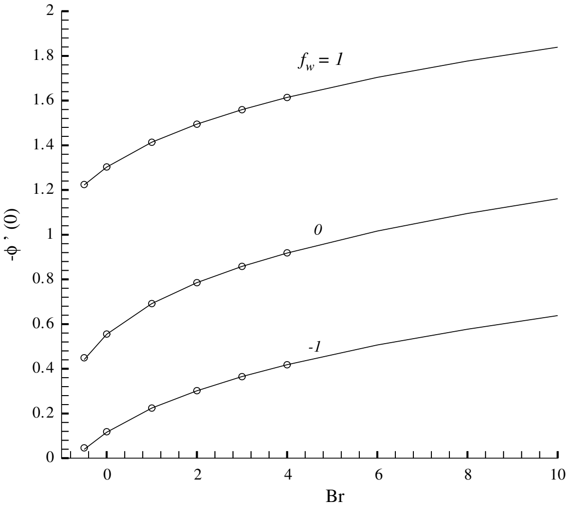

Fig. 9. The effect of buoyancy ratio Br on the Sherwood number when $Gr = 1$, $Le = 2$. Symbol: numerical results given by Murthy and Singh [26]; solid line: homotopy analysis results.

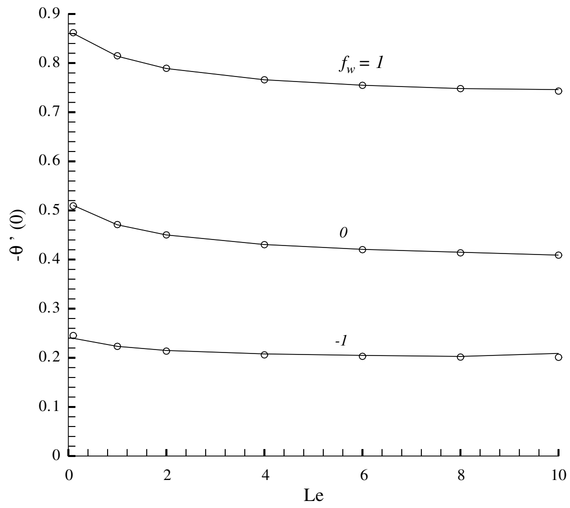

Fig. 10. The effect of Lewis number on the Nusselt number when $Gr = 1$, $Br = 1$. Symbol: numerical results given by Murthy and Singh [26]; solid line: homotopy analysis results.

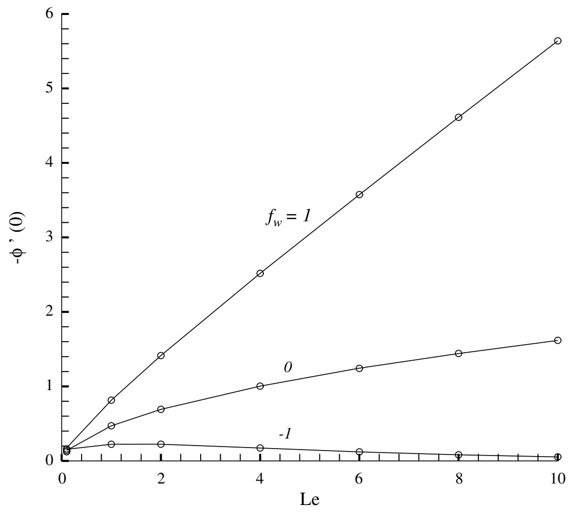

Fig. 11. The effect of Lewis number on the Sherwood number when $Gr = 1$, $Br = 1$. Symbol: numerical results given by Murthy and Singh [26]; solid line: homotopy analysis results.

References

[1] D.A. Nield, A. Bejan, Convection in Porous Media, second ed., Springer, New York, 1998.
[2] D.A. Nield, Onset of thermohaline convection in a porous medium, Water Resour. Res. 4 (1968) 553–560.
[3] A.A. Khan, A. Zebib, Double diffusive instability in a vertical layer of a porous medium, J. Heat Transfer 103 (1981) 179–181.
[4] J.Y. Jang, W.J. Chang, The flow and vortex instability of horizontal natural convection in a porous medium resulting from combined heat and mass buoyancy effects, Int. J. Heat Mass Transfer 31 (1988) 769–777.
[5] A. Raptis, G. Tzivanidis, N. Kafousias, Free convection and mass transfer flow through a porous medium bounded by an infinite vertical limiting surface with constant suction, Lett. Heat Mass Transfer 8 (1981) 417–424.
[6] A. Raptis, N. Kafousias, C. Massalas, Free convection and mass transfer flow through a porous medium bounded by

an infinite vertical porous plate with constant heat flux, ZAMM 62 (1982) 489–491.
[7] A. Bejan, K.R. Khair, Heat and mass transfer by natural convection in a porous medium, Int. J. Heat Mass Transfer 28 (1985) 909–918.
[8] A. Nakayama, M.A. Hossain, An integral treatment for combined heat and mass transfer by natural convection in a porous medium, Int. J. Heat Mass Transfer 38 (1995) 761–765.
[9] P. Singh, Queeny, Free convection heat and mass transfer along a vertical surface in a porous medium, Acta Mech. 123 (1997) 69–73.
[10] F.C. Lai, F.A. Kulacki, Coupled heat and mass transfer by natural convection from vertical surfaces in porous media, Int. J. Heat Mass Transfer 34 (1991) 1189–1194.
[11] R.S. Telles, O.V. Trevisan, Dispersion in heat and mass transfer natural convection along vertical boundaries in porous media, Int. J. Heat Mass Transfer 36 (1993) 1357–1365.
[12] D. Angirasa, G.P. Peterson, I. Pop, Combined heat and mass transfer by natural convection with opposing buoyancy effects in a fluid saturated porous medium, Int. J. Heat Mass Transfer 40 (1997) 2755–2773.
[13] O.V. Trevisan, A. Bejan, Natural convection with combined heat and mass transfer buoyancy effects in a porous medium, Int. J. Heat Mass Transfer 28 (1985) 1597–1611.
[14] O.V. Trevisan, A. Bejan, Mass and heat transfer by natural convection in a vertical slot filled with porous medium, Int. J. Heat Mass Transfer 29 (1986) 403–415.
[15] M. Hasan, A.S. Mujumdar, Transpiration-induced buoyancy effect around a horizontal cylinder embedded in a porous medium, Int. J. Energy Res. 9 (1985) 151–163.
[16] J.Y. Jang, W.J. Chang, Buoyancy-induced inclined boundary layer flow in a porous medium resulting from combined heat and mass buoyancy effects, Int. Commun. Heat Mass Transfer 15 (1988) 17–30.
[17] F.C. Lai, C.Y. Choi, F.A. Kulacki, Coupled heat and mass transfer by natural convection from slender bodies of revolution in porous media, Int. Commun. Heat Mass Transfer 17 (1990) 609–620.
[18] A.A. Raptis, Unsteady free convective flow and mass transfer through a porous medium bounded by an infinite vertical limiting surface with constant suction and time-dependent temperature, Int. J. Energy Res. 7 (1983) 385–389.
[19] J.Y. Jang, J.R. Ni, Transient free convection with mass transfer from an isothermal vertical flat plate embedded in a porous medium, Int. J. Heat Fluid Flow 10 (1989) 59–65.
[20] M. Kumari, G. Nath, Double diffusive unsteady free convection on two-dimensional and axisymmetric bodies in a porous medium, Int. J. Energy Res. 13 (1989) 379–391.
[21] I. Pop, H. Herwig, Transient mass transfer from an isothermal vertical flat plate embedded in a porous medium, Int. Commun. Heat Mass Transfer 17 (1990) 813–821.
[22] O.V. Trevisan, A. Bejan, Combined heat and mass transfer by natural convection in a porous medium, Adv. Heat Transfer 20 (1990) 315–352.
[23] M. Kumari, H.S. Takhar, G. Nath, Double diffusive non-Darcy free convection from two-dimensional and axisymmetric bodies of arbitray shape in a saturated porous medium, Indian J. Technol. 26 (1988) 324–328.
[24] J.Y. Jang, D.J. Tzeng, H.J. Shaw, Transient free convection with mass transfer on a vertical plate embedded in a high-porosity medium, Numer. Heat Transfer Part A 20 (1991) 1–18.
[25] S.K. Rastogi, D. Poulikakos, Double-diffusion from a vertical surface in a porous region saturated with a non-Newtonian fluid, Int. J. Heat Mass Transfer 38 (1995) 935–946.
[26] P.V.S.N. Murthy, P. Singh, Heat and mass transfer by natural convection in a non-Darcy porous medium, Acta Mech. 138 (1999) 243–254.
[27] S.J. Liao, The proposed homotopy analysis techniques for the solution of nonlinear problems. Ph.D. dissertation (in English), Shanghai Jiao Tong University, Shanghai, 1992.
[28] S.J. Liao, An approximate solution technique which does not depend upon small parameters: a special example, Int. J. Nonlinear Mech. 30 (1995) 371–380.
[29] S.J. Liao, A kind of approximate solution technique which does not depend upon small parameters (part 2): an application in fluid mechanics, Int. J. Nonlinear Mech. 32 (1997) 815–822.
[30] S.J. Liao, A uniformly valid analytic solution of two-dimensional viscous flow over a semi-infinite flat plate, J. Fluid Mech. 385 (1999) 101–128.
[31] S.J. Liao, An explicit, totally analytic approximate solution for Blasius' viscous flow problems, Int. J. Nonlinear Mech. 34 (1999) 759–778.
[32] S.J. Liao, An analytic approximation of the drag coefficient for the viscous flow past a sphere, Int. J. Nonlinear Mech. 37 (2002) 1–18.
[33] S.J. Liao, A. Campo, Analytic solutions of the temperature distribution in Blasius viscous flow problems, J. Fluid Mech. 453 (2002) 411–425.